

---

Article

Not peer-reviewed version

---

# Robust Daytime In Situ Target Strength Estimation of Pacific Hake (*Merluccius productus*) over a Wide Size Range

---

[Dezhang Chu](#) , [Stephane Gauthier](#) , [Stephen de Blois](#) <sup>\*</sup> , Julia Clemons , Rebecca Thomas

Posted Date: 1 October 2025

doi: [10.20944/preprints202510.0069.v1](https://doi.org/10.20944/preprints202510.0069.v1)

Keywords: hake; echosounder; in situ target strength; biomass estimate



Preprints.org is a free multidisciplinary platform providing preprint service that is dedicated to making early versions of research outputs permanently available and citable. Preprints posted at Preprints.org appear in Web of Science, Crossref, Google Scholar, Scilit, Europe PMC.

Copyright: This open access article is published under a Creative Commons CC BY 4.0 license, which permit the free download, distribution, and reuse, provided that the author and preprint are cited in any reuse.

Disclaimer/Publisher's Note: The statements, opinions, and data contained in all publications are solely those of the individual author(s) and contributor(s) and not of MDPI and/or the editor(s). MDPI and/or the editor(s) disclaim responsibility for any injury to people or property resulting from any ideas, methods, instructions, or products referred to in the content.

## Article

# Robust Daytime In Situ Target Strength Estimation of Pacific hake (*Merluccius productus*) Over a Wide Size Range

Dezhang Chu <sup>1</sup>, Stéphane Gauthier <sup>2,3</sup>, Stephen de Blois <sup>1,\*</sup>, Julia Clemons <sup>1</sup>  
and Rebecca Thomas <sup>1</sup>

<sup>1</sup> NOAA Fisheries, Northwest Fisheries Science Center, 2725 Montlake Blvd. E., Seattle, WA 98112, United States (\*Retired)

<sup>2</sup> Fisheries and Oceans Canada, Institute of Ocean Sciences, 9860 West Saanich Rd., Sidney, BC, V8L 4B2 Canada

<sup>3</sup> Department of Biology, University of Victoria, Victoria, Canada

\* Correspondence: author: steve.deblois@noaa.gov

## Abstract

Accurate determination of the target strength (TS) of a fish species is essential for estimating the biomass of fish stocks using acoustic technology. This study estimated the daytime *in situ* target strength of Pacific hake (*Merluccius productus*) at 38 kHz using echosounder data collected during hake biomass acoustic trawl surveys and research cruises conducted from 2009 to 2019 by U.S. and Canadian scientists. The intercept term for the 20-log TS regression over fish length at 38 kHz,  $b_{20}$ , was found to be -67.9 dB re 1 m<sup>2</sup> (CI: -68.09, -67.72) closely aligning with the currently used value of -68 dB in biomass assessments. Applying the revised  $b_{20}$  value of -67.9 dB in past stock assessments suggests that biomass estimates would be underestimated by less than 3%, which is well within the typical uncertainty range of fish stock assessments.

**Keywords:** hake; echosounder; *in situ* target strength; biomass estimate

---

## 1. Introduction

Effective management of fisheries and ecosystems requires marine scientists to take on substantial responsibilities, including monitoring, assessing, and researching marine resource distributions. Pacific hake (*Merluccius productus*), hereafter referred to as hake, is a commercially important marine fish found off the west coast of North America (Longo et al., 2024). Over the past decade (2014–23), coastwide annual harvests averaged 338,606 metric tons (Grandin et al., 2024), with U.S. and Canadian catches averaging 275,957 metric tons and 62,648 metric tons, respectively. In 2023, the coastwide catch reached 263,981 metric tons (Grandin et al., 2024). The U.S. West Coast's hake fishery, including non-tribal at-sea and shoreside operations, supported 4,450 jobs and generated an income of \$335 million in 2021.

Beyond its commercial significance, hake is a key trophic species and the most abundant groundfish in the California Current Large Marine Ecosystem (Sherman, 1991). Given its prominent economic and ecological value, integrated acoustic trawl (IAT) surveys have been conducted to assess hake's abundance, spatial and temporal distributions, and additional biological characteristics along the west coasts of the United States and Canada (Fleischer et al., 2005). These surveys began in 1977, with the Alaska Fisheries Science Center (AFSC) conducting triennial IAT surveys in U.S. and Canadian waters. In 1990, Fisheries and Oceans Canada (DFO) initiated annual IAT surveys in Canadian waters. After the 2001 survey, responsibility for the U.S. portion of the IAT survey transitioned to the Northwest Fisheries Science Center (NWFSC), and the survey frequency increased from triennial to biennial. Since 1995, the United States and Canada have collaborated on hake assessments. The triennial IAT surveys of 1995, 1998, and 2001 were conducted jointly by AFSC and

DFO, while surveys since 2003 have been conducted by NWFSC and DFO. The joint hake surveys normally began at Point Conception, California (the current southern extent of the survey area) and proceeded north along the west coast of the U.S. and Canada, surveying Queen Charlotte Sound, Hecate Strait (above Port Hardy in Fig.1), Dixon Entrance (the northern extent of the survey area, straddling the Canada and Alaska border), and the west side of Haida Gwaii, which was surveyed from north to south (Fig. 1, with the actual 2019 survey transects).

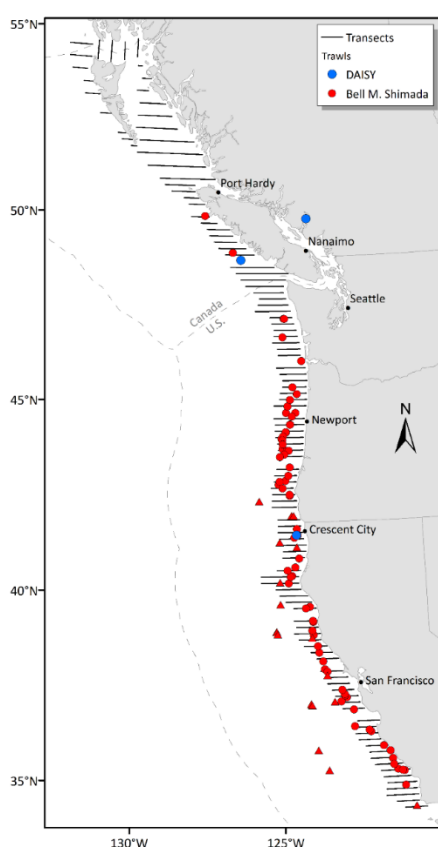


**Figure 1.** Survey area map and the locations of the biological trawls associated with the TS samples from individual hake used in this study (circles for summer trawls, triangles for winter trawls). The survey transects are for the actual 2019 hake survey and the inset is the photo of the DAISY deployed off the Canadian Coast Guard Ship (CCGS) W. E. Ricker.

Estimating the abundance or biomass of fish stocks using acoustic technology requires accurate measurements of an acoustic property known as target strength (TS). TS is directly tied to biomass estimates, which are based on echo integration theory (Scherbino and Truskanov, 1966). Conceptually, TS measures the acoustic energy scattered (typically in the backward direction) from an object relative to the source intensity (Medwin and Clay, 1998).

Three common methods are used to estimate the TS of fish: *in situ* field data (Ona, 1995; Gauthier and Rose, 2002; Peña, 2008; Kloster et al., 2011; Madirolas et al., 2017), *ex situ* data (Kang and Hwang, 2003; Henderson and Horne, 2007; Boswell and Wilson, 2008;), and theoretical model predictions (Love, 1978; Foote, 1985; Clay and Horne, 1994; Jech et al., 2015; Chu, 2024). The target strength currently used by NWFSC and DFO to estimate hake biomass was originally published by Traynor (1996). This value was derived from *in situ* hake echosounder data at 38 kHz using a widely accepted 20-log regression formula based on the theoretical relationship between the differential backscattering cross section ( $\sigma_{bs}$ ) and fish length ( $L$ )  $\sigma_{bs} \propto L^2$ . In the case of Pacific hake,  $L$  represents fork length. The TS is commonly expressed logarithmically as:

$$TS = 10 \log_{10} \sigma_{bs} = 20 \log_{10} L + b_{20} \quad (1)$$

where fish length is measured in centimeters, and the intercept term  $b_{20}$  is in dB re 1m<sup>2</sup>. The  $b_{20}$  that has been used by NWFSC/DFO for Pacific hake biomass estimates has been historically set to -68 dB based on *in situ* target strength values reported by Traynor (1996). However, this intercept value was questioned by Henderson and Horne (2007), where a much smaller  $b_{20}$  was suggested.

To address discrepancies in  $b_{20}$  estimates and evaluate the validity of the currently used  $b_{20}$ , we analyzed *in situ* echosounder TS data from single targets collected between 2009 and 2019 during hake biomass surveys and research cruises. In contrast to Henderson and Horne (2007), which used a combination of *ex situ* and nighttime *in situ* methods (similar to Traynor (1996)) to estimate target strength, this study focused on daytime *in situ* methods as being more representative of fish encountered during the daytime survey used for stock assessment, and also provided estimates of accuracy and robustness. To account for bias due to multiple target scattering and low signal to noise ratio (SNR) typically encountered during daytime surveys (when fish are found in denser aggregations at greater depth) we have used a stepwise approach for selecting valid targets and further introduced a pulse energy filtering method.

## 2. Materials and Methods

### 2.1. Data Description

Acoustic data were collected between 2009 and 2019 using EK60 split-beam echosounders manufactured by Kongsberg Simrad. This study focused on data collected at 38 kHz, the primary frequency used for hake biomass estimation and widely recognized for fish biomass assessments globally. Single-fish TS measurements were collected during midwater trawl verifications tows conducted at an average vessel speed of approximately 3 knots (~1.5 m/s) using the NOAA Fisheries Survey Vessel (FSV) *Bell M. Shimada*. Only trawls in which hake exceeded 95% of the total catch composition (by weight) were selected for TS analysis.

In addition, a Dropped Acoustic Information SYstem (DAISY), a deployable instrument, was used to collect echosounder data off the Canadian Coast Guard Ship (CCGS) *W. E. Ricker* (Inset in Fig. 1). DAISY consisted of 38-kHz and 120-kHz split-beam EK60 echosounders connected to a power supply inside a pressure housing. The unit was equipped with 200 m of cable for deployment at depth using a relay for topside control and included a heading, pitch, and roll sensor. The CCGS *W. E. Ricker* drifted while the DAISY was deployed to collect data. Each deployment of DAISY was associated with midwater verification trawl. Catches of hake from these trawls comprised 80%, 82%, and 99% of the total catch for September 7, 2014, September 14, 2014, and March 23, 2016, respectively. An in-trawl camera system indicated that the other species caught in 2014 (mostly opalescent inshore squid, *Doryteuthis opalescens*) were in different depth layers than the hake. The geographic locations of all selected trawls used for hake *in situ* target strength estimation are shown in Fig. 1. Echosounders from the Shimada and DAISY transmitted narrowband pulses with a duration of 1.024 ms. All echosounders were calibrated using the standard sphere method (Demer et al. 2015) prior to each survey, including the deployment of calibration sphere at depth for DAISY measurements.

### 2.2. Data Analysis

To correctly obtain single target TS data, the Single Target detection algorithm of Echoview (version 13.1) was used (Table 1). The single targets that fell within these parameters only served as foundation for further analysis. Originally, we used the fish tracking algorithm provided within Echoview (Table 2), based on the Alpha-Beta tracking algorithm described by Blackman (1986), but inspections revealed a high number of erroneous tracks which required substantial manual corrections, despite several attempts at fine-tuning the tracking parameters. To better ensure the TS samples in the selected fish tracks were from individual fish, we manually selected candidates from these fish tracks, following stringent guidelines to guarantee the quality of the samples for final TS analysis. The guidelines for single targets based on initial fish tracks analysis were:

1. Fish tracks were selected throughout the depth range of aggregations but primarily from the outskirts of fish aggregations away from regions of highest densities (generally the center of aggregations) to minimize potential biases from multiple-targets.
2. Each fish track had to contain at least five contiguous echoes.

3. Following track selection, only targets that were within 2° of the acoustic beam axis were retained for further analyses.

4. Sample TS values greater than -30 dB were excluded to eliminate larger, non-hake targets or potential multiple targets.

**Table 1.** EK60 echosounder parameters for Single Target Detection.

Single Target Detection	
General parameters	Parameter Value
TS Threshold (dB)	-60
Pulse length determination level (dB)	6.0
Minimum normalized pulse length	0.2
Maximum normalized pulse length	1.8
Beam compensation	
Beam compensation model	Simrad LOBE
Maximum beam compensation (dB)	12.0
Exclusion	
Maximum standard deviation of	
Minor-axis angles (deg)	2.0
Major-axis angles (deg)	2.0

**Table 2.** EK60 initial target tracking parameters.

Direction on a 3-d orthogonal frame	Major axis	Minor axis	Depth
$\alpha$	0.7	0.7	0.7
$\beta$	0.5	0.5	0.5
Exclusion distance (m)	4.0	4.0	0.4
Weights	30	30	40
Minimum number of single targets		3	
Minimum number of pings		3	
Maximum gap (pings)		1	

Following the selection of the TS samples satisfying these criteria, additional filtering was applied using a pulse-energy detection range on each single target. The reasoning of using this pulse-energy criterion was based on the concept that if the echoes from two targets (or multiple targets) were either in or out of phase but arrived at slightly different time, the resultant echo would be either elongated or shortened, respectively, but still within the Single Target Detection pulse duration window specified in Table 1. As a result, the combined and normalized pulse-energy over a time window of the transmit pulse duration would likely be either greater or less than the normalized transmit pulse-energy over the duration of the transmit pulse (1.024 ms in this study). The pulse energy ( $E_{pulse}$ ) was calculated as:

$$E_{pulse} = \int_0^T I(i) dt \quad (2)$$

where  $I(t)$  is the echo intensity, which is proportional to the volume backscattering coefficient,  $s_v = 10^{S_v/10}$ , where  $S_v$  is the volume backscattering strength. Since the absolute value of  $s_v$  depends on the target, we used a normalized  $s_v$  and the normalized pulse energy in the actual algorithm:

$$\hat{E}_{pulse} = \sum_{i=1}^{N_p} \hat{s}_v(i) \quad (3)$$

where  $N_p$  is the number of samples in each transmitted pulse (4 in the case of Simrad EK60 system) and  $\hat{s}_v = \frac{s_v(i)}{\max_{i=1, \dots, N_p} \{s_v(i)\}}$  is the normalized  $s_v$  of the pulse of interest. TS samples were retained if their pulse energy satisfied the relation:

$$\bar{E}_{theo} - 3 \sigma_{st} < \hat{E}_{pulse} < \bar{E}_{theo} + 3 \sigma_{st} \quad (4)$$

where  $\bar{E}_{theo}$  and  $\sigma_{st}$  are the theoretical mean and the standard deviation of the normalized echo energy, respectively, and were estimated based on the recorded waveform of the EK60 transmit pulse presented in Figure 2.30 in Demer et al. (2017). Since each pulse in the EK60 has four samples, the start of a (theoretical) echo was randomized within the first 256  $\mu$ s time window of the pulse (equivalent to 1/4 of a 1024  $\mu$ s pulse length). 10,000 realizations of this randomized start time were used in estimating the theoretical  $\bar{E}_{theo}$  and  $\sigma_{st}$  with values of 3.56 and 0.14, respectively.

Biological catch data were matched with acoustic data by assigning the mean fork length from each trawl to corresponding single-fish TS samples. Only trawls in which the fork length distribution of hake was relatively unimodal and had a standard deviation of less than 5 cm were retained for analyses.

Representative echograms illustrating single-target detections are shown in Fig. 2, where the trawl traces were superimposed onto the echogram (Fig. 2a) and the chosen TS samples from single fish were away from the center of the fish aggregation, the region with the highest fish density. The single-fish TS were much easier to determine from the echograms collected with DAISY due to the slow vessel speed (Fig. 2b). As a result, the detected single-fish TS echo-traces were much longer than those collected when trawling at a ship speed of about 3 kts ( $\sim 1.5$  m/s).

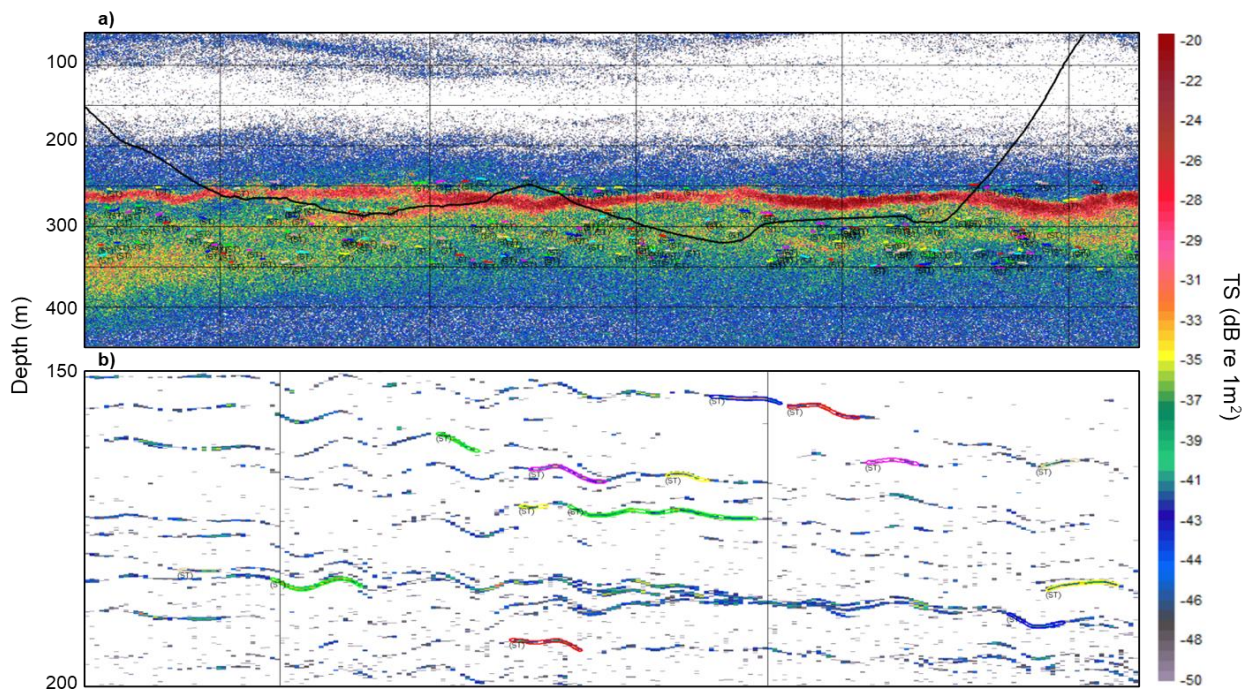


**Figure 2.** Examples of the Target Strength echograms from assumed individual hake, where each colored line (polygons) indicates an individual track. (a) Collected from the U.S. Fisheries Survey Vessel (FSV) *Bell M. Shimada* during a trawl (trawl path is indicated by the thick black line). Each vertical bar indicates 0.5 nmi; (b) DAISY drift TS echogram deployed from the CCGS *W. E. Ricker*, each vertical line representing 100 pings. Depth (in m) is indicated on the left side.

### 2.3. Estimation of $b_{20}$

To obtain an optimized estimate of the intercept,  $b_{20}$ , we used the least-square fit to the TS data using Eq. (1), a 20-log form of the TS-length regression relation. The mean fork length (from trawl samples) was categorized in 1 cm length bins. Since the only unknown is the intercept term  $b_{20}$ , it is straightforward to show that using the standard least-square approach,  $b_{20}$  can be estimated by

$$b_{20} = \frac{\sum_{i=1}^{n_L} \sum_{j=1}^{n_{iL}} (TS_{ij} - 20 \log_{10} L_{ij})}{\sum_{i=1}^{n_L} n_{iL}} \quad (5)$$

where  $n_L$  is the total number of length bins and  $n_{iL}$  is the number of length samples in each length bin (which may have included more than one trawl when their mean length was within the

same 1 cm bin).  $TS_{ij}$  and  $L_{ij}$  are the measured TS (dB) value and the corresponding hake fork length (cm) for the  $i^{\text{th}}$  length bin and  $j^{\text{th}}$  TS sample in the  $i^{\text{th}}$  length bin, respectively. For comparison, the TS-length regression was also assessed empirically with a free slope parameter in the form of:

$$TS = a \log_{10} L \text{ (cm)} + b_a \quad (6)$$

Where  $a$  is the slope parameter and  $b_a$  its associated intercept.

#### 2.4. Statistical Analysis

To evaluate the variability and robustness of the  $b_{20}$  estimate, three statistical methods were applied and compared. Each methods provide a slightly different perspective on the sampled data and their reliability:

1. Resampling: all TS data were randomly resampled with non-replacement, using 95%, 90%, and down to 5% of the original data, with 1,000 realizations for each percentage bracket. This addresses the sensitivity of the data to marginally high or low TS samples (or specific to trawl hauls) by assessing significant divergence in slope estimates as the TS sample size is gradually reduced down to a small fraction of all available data. This resampling approach also helps in identifying potential bias due to outliers, or disproportionate weight to sample values that are at the tail end of the distribution (e.g., hauls with the smallest and largest mean fork lengths).
2. Bootstrapping: The bootstrap method estimated the sampling distribution of  $b_{20}$  by resampling the original data using all (100%) data samples with replacement (Horowitz, 2019; Efron and Tibshirani, 1993), also with 1,000 realizations.
3. Jackknife: The jackknife cross-validation technique, a leave-one-out resampling method with replacement, was used for bias and variance estimation (Jones, 1974).

### 3. Results and Discussion

#### 3.1. Target Strength (TS) Data Processing and Acceptance

After applying the Single Target Detection and tracking criteria specified in Tables 1 and 2, the manual selection guidelines, and a pulse-energy filter, the processed TS samples were analyzed. The accepted TS samples from assumed single targets associated with the selected hauls across different years are summarized in Table 3. The dataset comprises a total of 92 hauls from 13 surveys conducted between 2009 and 2019, with an overall acceptance rate of single targets less than 2%. This was largely due to the pulse energy filter, which we found necessary to analyze target at long range in low signal to noise ratio conditions, because of the relatively high density of hake (and other scatterers) at depth during daytime surveys. The average biological catch per haul was approximately 380 kg, with an average hake catch composition of 98%, confirming that the samples were representative of hake-dominated areas. Exceptions were two hauls in 2014 that were associated with the DAISY data, where hake catch proportions were slightly above 80% (Table A1). Although the hake catches were lower for these DAISY data, the non-hake catches were primarily squids (no gas inclusions) and small lanternfish ( $\sim 5$ -cm), whose TS were believed to be much less than those of hake ( $L \geq 17$  cm, Figs. 7 and 8). Furthermore, in-trawl camera footage indicated that these non-hake animals were caught at different depths from hake, as explained in Sec. 2.1.

**Table 3.** Information of target strength (TS) samples from the targets associated with the chosen midwater trawl hauls. The average catch weight per haul was 377 kg and the average hake catch was 97%.

Dataset	No. Hauls	TS Samples (original)	TS Samples (Pulse-energy filtered')
2009	8	6891	150
2011	7	4875	98
2013	12	14103	241
2014	2	1898	6
2015	9	1915	48
2016 Winter	13	9922	218

2017 Winter	9	4158	92
2017 Summer	5	3365	61
2018	2	216	5
2019	22	16829	481
DAISY 2014-09-07	1	3722	40
DAISY 2014-09-12	1	3788	47
DAISY 2016-03-23	1	5372	23
<b>Sum</b>	<b>92</b>	<b>77054</b>	<b>1510</b>

### 3.2. TS Distribution and Depth Analysis

The histogram of the TS samples from detected single targets is shown in Fig. 3. The TS distribution was not symmetric around the mean or mode, approximately at -37.5 dB. A small portion of the TS samples had very low TS values, indicating the TS samples were either from smaller hake individuals, from hake that had larger tilt angles, or from small non-hake targets. Although the lower limit of the Single Target Detection algorithm was specified at -60 dB re 1 m<sup>2</sup>, the actual accepted TS samples following the filtering processes were all greater than -55 dB re 1 m<sup>2</sup>.

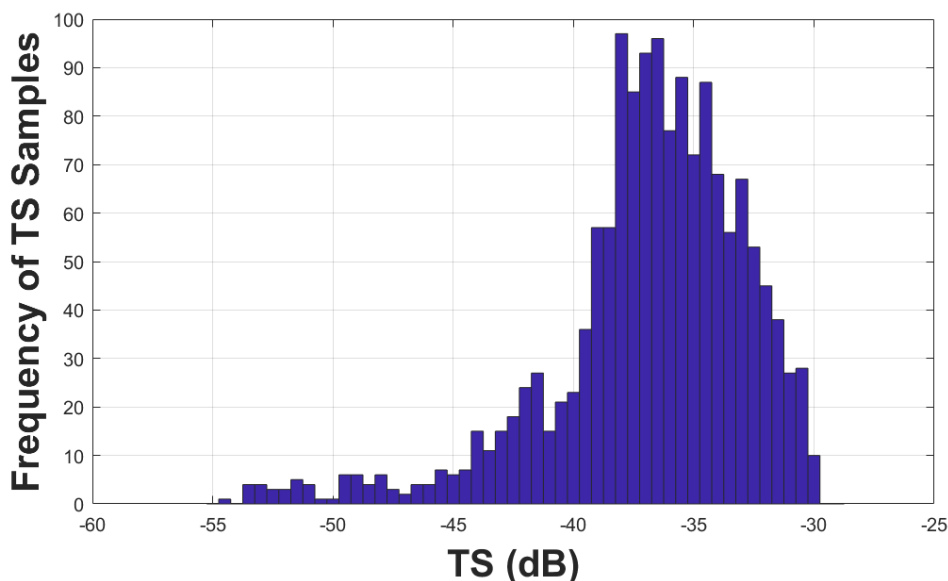


**Figure 3.** Histogram of the TS from single targets.

TS samples distributed between 150 and 400 m represented about 80% of the total accepted TS values (Fig. 4). There were few samples detected in very shallow water, i.e., shallower than 100 m depth, but their corresponding TS values were mostly lower than -45 dB re 1 m<sup>2</sup>, significantly lower than the mean TS value of -36.8 dB re 1 m<sup>2</sup>, or the median value of -36.3 dB re 1 m<sup>2</sup> (Fig. 5), likely from smaller age-1 juvenile hake, or even age-0 young-of-year (YOY) hake.

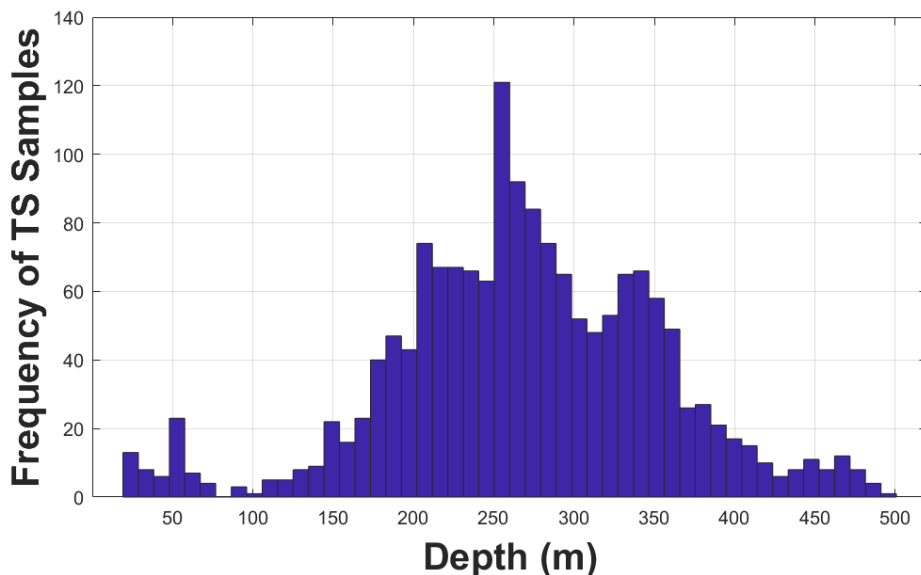


**Figure 4.** Histogram of the TS from single targets as a function of target depth.

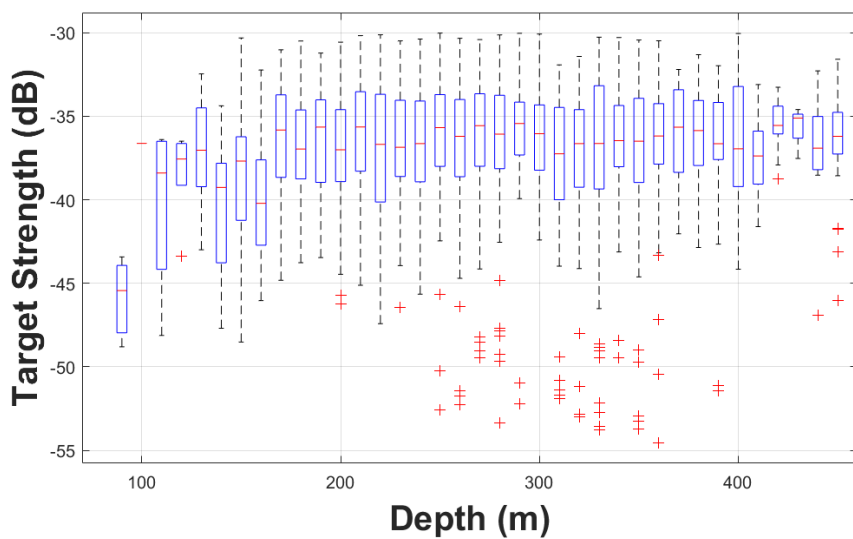


**Figure 5.** Target strength (TS) from single targets as a function of depth, where the central mark (red line) is the median, the edges of the box (blue) are the 25th and 75th percentiles, the whiskers (black dashed line) extend to the most extreme data points (red plus) that the algorithm considers to be not outliers, and these outliers are plotted individually.

### 3.3. Spatial Variability and Fork Length Association

Except for TS samples around lat 43.5°N, where the TS values were lower and more spread out, all TS samples had median values close to the overall median of -36.9 dB re 1 m<sup>2</sup> (Fig. 6). These low TS values at lat 43.5°N possibly correspond to the smaller hake fork length at the same latitude (Fig. 7) as stated in Section 3.2. Some trawls at the median length were at the higher end of the 75<sup>th</sup> percentile (lat 36.5°N, 38.5°N, 39°N, 41°N, and 43.5°N), or at the lower end of the 25<sup>th</sup> percentile (lat 37.5°N, 42°N, 42.5°N, and 44°N). At some latitudes, the 25<sup>th</sup> and 75<sup>th</sup> percentiles and the median were identical (lat 41.5°N and 45.5°N), indicating that the catches were uniform in length distribution.

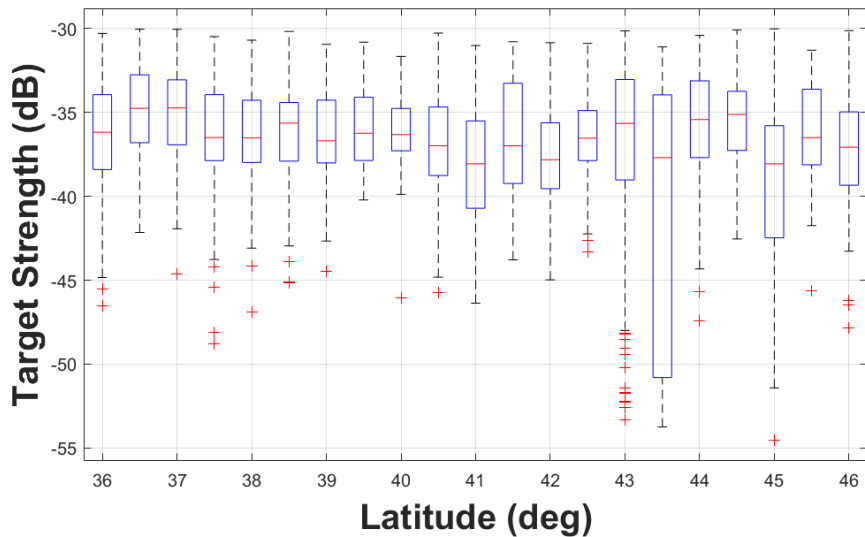


**Figure 6.** Target strength (TS) from single targets as a function of latitude.

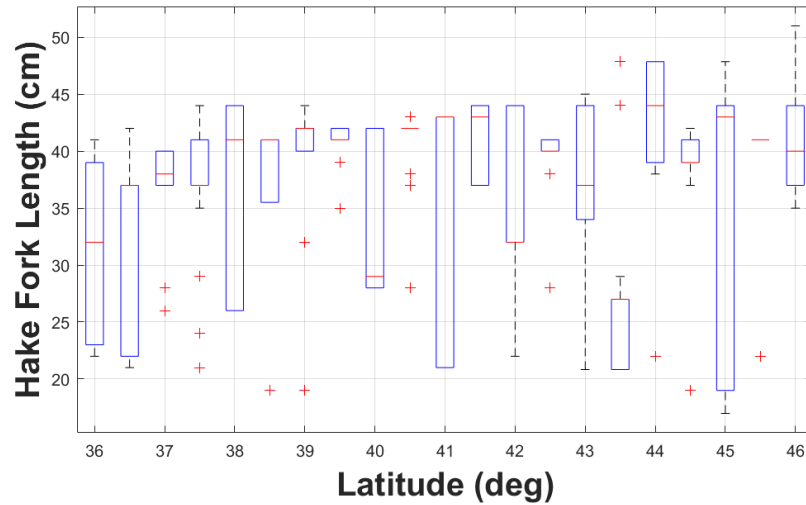


**Figure 7.** Hake fork length from biological haul catches as a function of length.

### 3.4. TS-Length Regression

One of the most important results of this study is the regression of TS versus length. The regression was performed in the logarithmic domain for TS (dB) and linear domain for the length (cm) (Sec. 2.3). The boxplot of the TS values of the accepted samples as a function of length is presented in Fig. 8. Mean length from trawls were categorized in 1 cm length bins, which may include samples from more than one trawl (when their mean length was similar). The 20-log regression formula with a  $b_{20}$  of -67.9 dB is only 0.1 dB larger than the value derived from Traynor et al. (1996) currently used for biomass estimates of Pacific hake. Since the areal acoustic scattering coefficient (NASC) is used for converting the acoustic quantity to biological quantity, i.e., the number of fish:

$$N = \frac{\text{NASC}}{\sigma_{bs}} \quad (7)$$

where  $\sigma_{bs}$  is the differential scattering cross section defined in Eq. (1), or  $\sigma_{ba} = 10^{TS/10}$ . For a fixed NASC value, difference in  $\sigma_{bs}$  will result in a change in number of fish,  $N$ :

$$\Delta N = -\frac{\text{NASC}}{\sigma_{bs}^2} \Delta \sigma_{bs} \quad (8)$$

A relative change in estimated fish number is the ratio of (8) to (7):

$$\frac{\Delta N}{N} = -\frac{\Delta \sigma_{bs}}{\sigma_{bs}} = -\Delta TS \frac{\log_e 10}{10} \approx -0.23\Delta TS \quad (9)$$

As a result, a 0.1 dB increase in TS would lead to less than 3% ( $\Delta N/N \approx -0.23 < 3\%$ ) in estimated fish number. Applying this revised value and assuming that the fish weight is proportional to fish number, the estimated biomass would have been less than 3% higher than the acoustic biomass estimates reported from previous Joint U.S.-Canada IAT Surveys (Grandin et al., 2024).

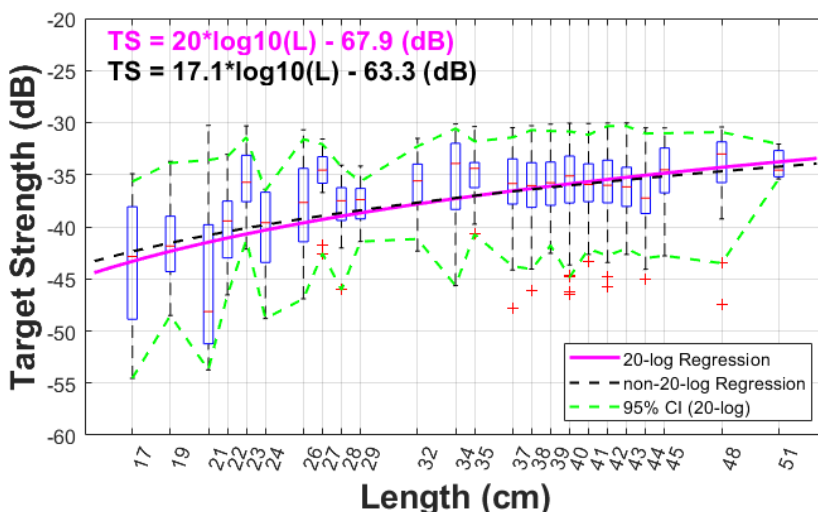


**Figure 8.** Target strength (TS) from single targets as a function of length. The x-axis is marked and labelled at the mean fork length of the samples. The fitted TS-length regression (solid magenta line) is superimposed onto the plot, and the upper and lower 95% Confidence Intervals of the samples values in each length category are plotted with a dashed line (dashed green line). A non-20-log regression (dashed black) is also superimposed to the plot.

As a comparison, a linear regression where slope was estimated was also performed, resulting in a slope of 17.1 and the intercept of -63.3 dB. This regression curve is also shown in Fig. 8 (dashed black line), which is not very different from the 20-log regression curve (solid magenta line) and well within the samples confidence interval that includes the 20-log. This non-20-log regression relation was an empirical data fit comparison. For gadoids, which have large spheroid-shape swimbladders, the relationship is justified to follow a 20 log relationship (Lauffenburger et al., 2023). Scattering physics reveals that the differential backscattering cross section in the farfield (i.e., plane wave incidence) should be proportional to the squared length of the target of finite size (i.e., smaller than the first Fresnel zone) (Morse and Ingard, 1968; Simmonds and MacLennan, 2005; Stanton, 1988, 1989). There has been debates in the literature that the relationships of target strength to length does not always necessarily follow a 20 log regression (McClatchie et al., 1996, 2003), perhaps due to complexity in fish body types and swimbladder morphologies.

### 3.5. Statistical Robustness of $b_{20}$

To assess the robustness and the variability of the value of  $b_{20}$  in the TS-length regression, we performed the three statistical processes as described in Sec. 2.2, i.e., partial, Bootstrapping, and Jackknife resampling methods, all with 1,000 iterations.

a. Partial sampling: For the partial sampling, we resampled the whole data population with 95% down to 5% in 5% increments, and at each percentage value we performed the resampling with replacement 1,000 times or realizations. The results are tabulated in Table 4 and their graphic representation is shown in Fig. 9. All distributions from the resampling can be well described by Gaussian or Normal distributions. A representative example at 90% resampling is illustrated in Fig. 10, where a Gaussian Probability Density Function (PDF) with a mean of -67.9 dB and standard deviation of 0.03 dB is superimposed onto the plot of the raw resampled values. Note that even with

a substantially low number of selected TS samples at 5% of the original data, the estimated mean value of the *in situ* TS was only 0.003 dB lower than -67.9 dB.

b. Bootstrapping: Bootstrapping yielded a  $b_{20}$  mean of -67.9 dB with a 95% confidence interval of [-68.09, -67.72]

c. Jackknife analysis also resulted in a  $b_{20}$  mean of -67.9 dB with a standard deviation of 0.002 dB.

**Table 4.** Results from the partial resampling with replacement.

Resample Percentage	Mean (dB)	Standard Deviation (dB)
5%	-67.9	0.42
10%	-67.9	0.29
20%	-67.9	0.19
30%	-67.9	0.15
40%	-67.9	0.12
50%	-67.9	0.10
60%	-67.9	0.08
70%	-67.9	0.06
80%	-67.9	0.05
85%	-67.9	0.04
90%	-67.9	0.03
95%	-67.9	0.02

These analyses all confirm the robustness of the  $b_{20}$  estimate, with minimal variability, well within the tolerance uncertainty in the stock assessment (Grandin et al., 2024). The low variability observed in the data indicate consistency in TS measurements, likely the result of the extensive filtering of data, primarily based on the last step involving the pulse energy filter.

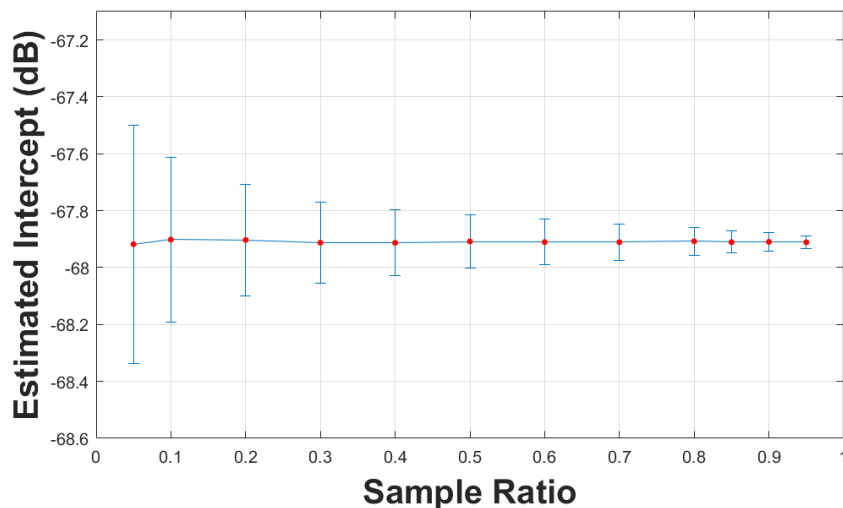


**Figure 9.**  $b_{20}$  estimates from Bootstrapping resampling with 5% to 95% of original TS samples, where 1,000 realizations were used.

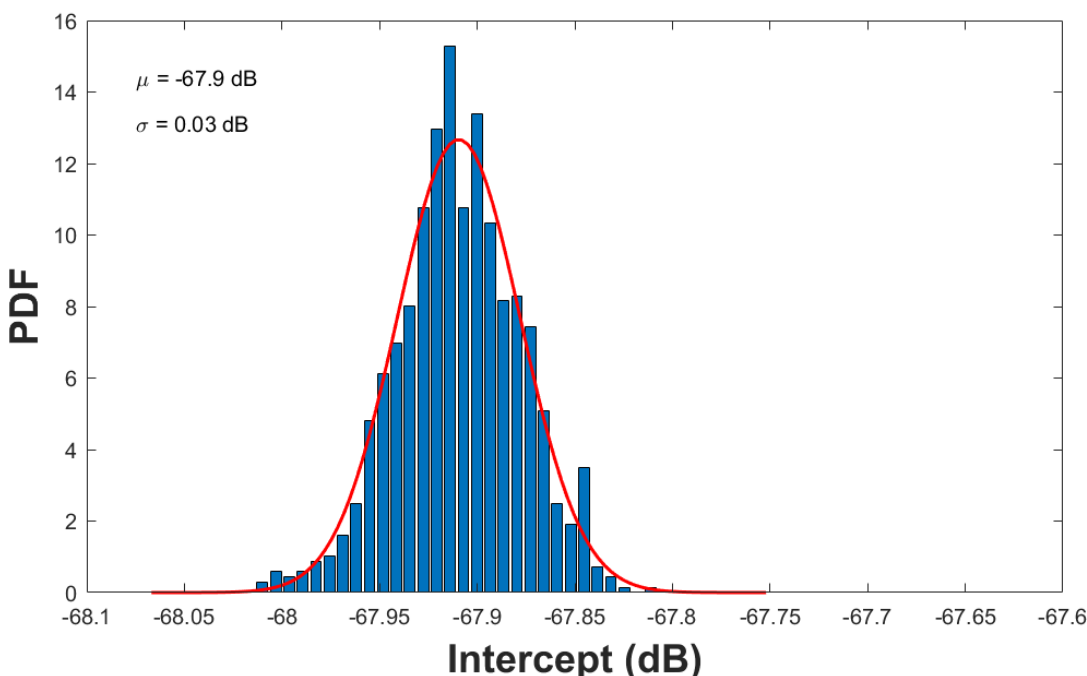


**Figure 10.**  $b_{20}$  estimate from partial resampling with 90% of the whole TS sample population, where 1,000 realizations were used. The parameters  $\mu$  and  $\sigma$  are the mean and standard deviation of the Gaussian PDF (red solid line).

### 3.6. Comparison with Previous Studies

Although the  $b_{20}$  value reported here is similar to that of Traynor (1996), it was 4–6 dB higher than that reported by Henderson and Horne (2007). Several factors may explain this discrepancy:

a. Data Collection Conditions: previous studies on Pacific hake used TS data collected at night, while all of the data presented in this paper were collected during daytime, i.e., consistent with the hake survey time from sunrise to sunset (Clemons et al., 2024). Hake TS measurements during daylight are more representative for biomass estimation as hake aggregates at depth during the day, but tend to scatter at night when there are less visual cues. As hake scatter and spread out through the water column at night they could present increased tilt angles, resulting in reduced TS values.

b. Length Range and Regression Consistency: Henderson and Horne's *ex situ* TS data spanned a narrow fork length range (44–53 cm), with TS values spread over an 8 dB range (Fig. 8 in Henderson and Horne, 2007), potentially reducing regression reliability and robustness.

c. Backscatter Model Discrepancies: The Kirchhoff Ray-Mode (KRM, Clay and Horne, 1994) backscatter model used by Henderson and Horne, with X-ray images of fish bodies and the swimbladders of live fish captured at sea, showed predictions 4–6 dB higher than their *ex situ* TS measurements (Fig. 6a in Henderson and Horne, 2007), indicating inconsistencies between model predictions and the *ex situ* measurements, but consistent with the findings from this study.

Results from these *in situ* measurements are consistent with the findings of Traynor (1996) despite their relatively small dataset of target strength measurements. The intercept value of -67.9 dB is in line, but lower by ~2 dB than reported for other gadoids (Rose and Porter, 1996, Pedersen et al., 2011, Lauffenburger et al., 2023). Consistency and low variability in TS measurements values observed over nine surveys (spanning 10 years) provide confidence in the use of the -68 dB intercept value currently used for Pacific hake biomass estimates obtained from acoustic surveys.

### 3.7. Limitations of the Study

Collection of Pacific hake *in situ* target strength data during the day is problematic because these fish tend to aggregate at high densities in relatively deep waters (often mixed with other smaller mesopelagic scatterers), making collection of ship-based data prone to multiple target bias. Collection made at shorter range, for example using the DAISY system, partially addresses this issue, but are

resource demanding (requiring dedicated time and equipment). On the other hand, data collected during assessment and research surveys provide large volumes of data that can be mined afterward (see Lauffenburger et al., 2023 for another example). Because of the low signal to noise ratio conditions encountered in Pacific hake aggregations, selection of targets based on fish or target density metrics (Sawada et al. 1993, Gauthier and Rose, 2001), even at reduced survey speeds, were not used in this study (as very little data would be preserved). Rather, a stepwise approach to selection of targets was adopted, with the addition of a novel filter based on pulse energy used on the final dataset. The consistency of TS values obtained (especially when compared to closer measurements made with DAISY) provide further evidence for the validity of this approach. It is also important to note that ship-based target strength measurements in this study were all made during midwater trawling operations (because of the reduced vessel speed). There is evidence that trawling affect fish behavior (Winger et al., 2010). Acoustic data collection from the centerboard of the vessel were made prior to the trawl going through the aggregation, but increased vessel and trawling gear noise may have an impact on the orientation and swimming behavior of fish. There is however little evidence of change in aggregation characteristics and depth distribution prior compared to during trawling, so we are assuming that these measurements of target strength data were made on fish representative of those encountered during routine acoustic surveys.

#### 4. Conclusion

Single-fish TS data of Pacific hake at 38 kHz from more than ten surveys and research cruises spanning ten years were analyzed. These data were processed with a number of filters and criteria to ensure data quality so that all accepted TS samples were expected to be from individual hake. All echosounder data sets were verified by biological trawl catches with an average hake composition of more than 95% by weight to ensure the echoes were most likely from hake. The TS-length regression of 20-log linear representation, i.e., Eq. (1), suggests an intercept term,  $b_{20}$  of -67.9 dB, only 0.1 dB larger than the value currently used in acoustic biomass estimates. The updated  $b_{20}$  aligns closely with current biomass estimation practices, ensuring accuracy well within acceptable uncertainty limits. The results from three statistical validation methods, i.e., partial, Bootstrapping, and Jackknife resampling procedures, were used to assess the variability of the estimated  $b_{20}$ , ensuring accuracy within acceptable uncertainty limits while addressing discrepancies with earlier studies. These findings emphasize the importance of standardized sampling protocols and robust methods for advancing acoustic biomass assessment.

**Acknowledgments:** This project was supported by NOAA Fisheries and DFO. We acknowledge Chelsea Stanley and George Cronkite for their assistance with DAISY. Other members of the Fisheries Engineering and Acoustic Technologies team (NOAA/NWFSC) and DFO, Alicia Billings, John Pohl, Larry Hufnagle, Elizabeth Phillips, and Christopher Grandin helped in acoustic and biological data collections.

**Table A1.** Detailed catch information of all hauls used in this study.

Year	Haul Number	Latitude (deg North)	Longitude (deg West)	Mean fork length (cm)	Standard Deviation of fork length (cm)	CV (%)	# of length samples	Total catch (kg)	% of hake by weight
Shimada									
2009	8	37.0401	122.6764	40	3.76	9.4%	324	321	95%
2009	22	39.0280	123.9685	40	2.58	6.5%	347	1,426	100%
2009	39	42.7018	124.7260	38	2.34	6.2%	437	4,590	100%
2009	56	44.2032	124.9930	42	2.12	5.0%	301	1,100	99%
2009	57	44.3706	124.8315	41	2.5	6.1%	288	446	100%
2009	62	44.8783	124.4680	19	1.64	8.6%	336	1,749	100%
2009	64	44.8796	124.8209	43	2.52	5.9%	248	128	99%
2009	66	45.3749	124.4020	41	2.48	6.0%	339	268	100%

2011	2	35.3790	121.0993	22	1.25	5.7%	242	82	99%
2011	4	35.7137	121.4605	23	1.13	4.9%	280	941	100%
2011	9	37.3658	122.9050	24	1.88	7.8%	208	18	100%
2011	18	39.3728	123.9755	35	2.00	5.7%	276	116	100%
2011	27	44.3747	124.8392	39	2.96	7.6%	307	216	99%
2011	40	46.8773	124.9192	37	1.83	5.0%	264	259	100%
2011	44	47.3707	124.8633	38	1.93	5.1%	325	140	100%
2013	5	35.4248	121.3085	35	1.00	2.9%	118	33	99%
2013	10	35.9212	121.5310	26	1.42	5.5%	317	463	100%
2013	13	36.5982	122.6653	37	1.56	4.2%	308	181	100%
2013	16	37.2632	123.0873	37	1.72	4.7%	536	177	99%
2013	18	37.4207	122.9600	37	1.54	4.2%	333	495	100%
2013	33	40.5868	124.6773	38	2.24	5.9%	556	198	98%
2013	38	41.5960	124.5763	37	1.56	4.2%	414	369	100%
2013	42	43.0928	124.8732	37	1.94	5.2%	397	259	98%
2013	45	43.9313	124.9667	38	2.15	5.7%	345	446	100%
2013	48	44.2608	124.9428	39	2.69	6.9%	230	86	100%
2013	56	46.2453	124.2052	40	2.97	7.4%	353	318	97%
2013	76	50.0928	128.0172	51	3.62	7.1%	537	522	89%
2014	15	43.8840	124.7910	43	3.16	7.3%	237	642	100%
2014	16	43.8858	124.7343	44	3.35	7.6%	200	192	100%
2015	9	36.4460	122.1363	23	2.22	9.7%	373	49	98%
2015	13	37.4495	122.9712	22	1.46	6.6%	285	431	88%
2015	15	38.1177	123.6143	24	1.06	4.4%	375	69	94%
2015	21	39.7728	124.0748	35	3.40	9.7%	418	166	100%
2015	39	43.4477	124.7072	24	1.36	5.7%	323	1,316	100%
2015	42	43.7828	124.9052	42	1.56	3.7%	62	34	96%
2015	46	44.7827	124.6060	21	1.23	5.9%	481	290	100%
2015	60	47.3663	124.8485	23	2.02	8.8%	237	314	99%
2015	73	49.1188	126.8678	44	2.37	5.4%	288	156	100%
2016 Winter	2	42.1750	124.6632	29	2.74	9.4%	235	35	92%
2016 Winter	4	41.3485	124.4978	27	1.58	5.9%	474	440	93%
2016 Winter	7	41.4722	125.0988	44	2.72	6.2%	195	234	96%
2016 Winter	8	40.4218	125.0995	44	3.04	6.9%	221	460	100%
2016 Winter	9	39.8428	125.0960	44	3.02	6.9%	123	61	97%
2016 Winter	10	39.1192	125.2397	43	2.55	5.9%	256	141	85%
2016 Winter	11	39.1202	125.2287	43	2.59	6.0%	256	118	99%
2016 Winter	13	37.9578	123.5278	28	1.67	6.0%	210	125	96%
2016 Winter	18	37.2152	124.0930	42	3.01	7.2%	211	237	100%
2016 Winter	21	35.9870	123.8852	43	2.43	5.7%	235	139	92%
2016 Winter	29	37.1723	124.0630	42	2.99	7.1%	231	332	98%

2016 Winter	30	39.0515	125.1992	42	3.00	7.1%	200	225	99%
2016 Winter	32	42.5568	125.8293	44	2.75	6.3%	287	143	97%
2017 Summer	1	34.9915	121.0798	26	2.14	8.2%	331	37	98%
2017 Summer	4	36.4908	122.1897	28	2.15	7.7%	415	1,163	98%
2017 Summer	10	38.3297	123.6627	37	2.39	6.5%	395	531	98%
2017 Summer	14	39.1445	124.0088	38	2.30	6.1%	403	351	95%
2017 Summer	16	40.8132	124.5613	40	2.90	7.3%	419	316	91%
2017 Summer	19	41.6540	124.4612	27	1.91	7.1%	250	90	99%
2017 Summer	20	41.8235	124.4860	28	1.87	6.7%	242	586	100%
2017 Summer	25	42.9898	125.1188	41	2.92	7.1%	226	119	95%
2017 Summer	31	44.1580	124.9715	39	2.76	7.1%	396	202	98%
2017 Winter	3	42.1720	124.5940	19	1.28	6.7%	156	51	96%
2017 Winter	4	37.2585	123.3062	35	2.22	6.3%	201	123	93%
2017 Winter	6	35.4527	123.5482	43	3.21	7.5%	191	99	100%
2017 Winter	7	34.4397	120.7680	21	1.07	5.1%	401	100	100%
2017 Winter	12	38.9510	124.0153	34	1.67	4.9%	301	1,080	100%
2018	18	44.5778	124.6725	41	2.81	6.9%	245	378	100%
2018	19	44.5685	124.6752	43	2.67	6.2%	236	156	97%
2019	7	35.3937	121.1582	22	1.26	5.7%	212	52	100%
2019	8	35.5583	121.4342	23	1.69	7.3%	212	104	99%
2019	12	36.0648	121.7403	24	2.44	10.2%	220	87	97%
2019	19	37.5640	123.0483	32	2.32	7.3%	356	178	100%
2019	22	38.0565	123.5303	42	3.70	8.8%	349	525	99%
2019	24	38.5600	123.7883	38	3.01	7.9%	322	121	94%
2019	25	38.7320	123.8278	39	3.17	8.1%	334	141	100%
2019	29	39.4012	123.9842	40	2.25	5.6%	326	182	92%
2019	30	39.7312	124.2135	41	2.22	5.4%	441	210	98%
2019	33	40.3948	124.7948	41	2.07	5.0%	403	413	100%
2019	35	40.5643	124.7252	41	2.68	6.5%	438	612	99%
2019	36	40.7295	124.8352	41	2.57	6.3%	468	648	100%
2019	38	41.0465	124.4185	42	2.83	6.7%	373	393	100%
2019	45	42.7263	124.7283	42	3.23	7.7%	381	1,567	100%
2019	46	42.8943	124.9795	42	2.99	7.1%	366	576	100%
2019	47	43.0708	125.0855	42	2.54	6.0%	235	115	97%
2019	48	43.2257	124.7650	42	2.47	5.9%	343	313	100%
2019	50	43.7210	125.0668	43	2.44	5.7%	215	111	100%
2019	54	44.0552	124.9563	41	2.73	6.7%	381	701	99%

2019	56	45.0540	124.7597	44	1.97	4.5%	83	46	97%
2019	57	45.2223	124.6620	43	2.02	4.7%	276	148	97%
2019	59	45.5570	124.5612	45	2.12	4.7%	184	107	97%
<b>DAISY</b>									
9/7/2014	36	41.6582	124.5003	29	1.25	4.3%	101	259	80%
9/12/2014	41	48.9242	126.5505	48	3.41	7.1%	174	161	82%
3/23/2016	30	50.0170	123.9078	33	4.70	14.2%	150	29	99%
Mean		41.0717	124.1269	36.2	2.34	6.5%	299	379	98%

## References

1. Blackman, S. S., 1986. Multiple-target tracking with radar applications. Artech House.
2. Chu. D., 2024. Development and Application of Advanced Science and Technology in Fisheries Acoustics. *J. Marine Acoust. Soc. Jpn.* 51(4): 117-149.
3. Clay, C. S., and Horne, J. K., 1994. Acoustic models of fish: The Atlantic cod (*Gadus morhua*). *J. Acoust. Soc. Am.* 96: 1661–1668.
4. Clemons, J. E., S. Gauthier, S. K. de Blois, A. A. Billings, E. M. Phillips, J. E. Pohl, C. P. Stanley, R. E. Thomas and E. M. Beyer. 2024. The 2023 Joint U.S.–Canada Integrated Ecosystem and Pacific Hake Acoustic Trawl Survey: Cruise Report SH-23-06. U.S. Department of Commerce, NOAA Processed Report NMFS-NWFSC-PR-2024-01.
5. Demer, D. A., Andersen, L. N., Bassett, C., Berger, L., Chu, D., Condiotto, J., Cutter, G. R., *et al.* 2017. 2016 USA–Norway EK80 Workshop Report: Evaluation of a wideband echosounder for fisheries and marine ecosystem science. ICES Cooperative Research Report No. 336. 69 pp. <http://doi.org/10.17895/ices.pub.2318>.
6. Efron, B. and Tibshirani, R., 1993. An Introduction to the Bootstrap. Boca Raton, FL: Chapman & Hall/CRC. ISBN 0-412-04231-2.
7. Efron, B., 2003. Second thoughts on the bootstrap (PDF). *Statistical Science.* 18(2): 135–140. doi:10.1214/ss/1063994968
8. Fleischer, G. W., Cooke, K. D., Ressler, P. H., Thomas, R. E., de Blois, S. K., Hufnagle, L. C., Kronlund, A. R., Holmes, J. A., and Wilson, C. D., 2005. The 2003 integrated acoustic and trawl survey of Pacific hake, *Merluccius productus*, in U.S. and Canadian waters off the Pacific coast. U.S. Department of Commerce, NOAA Technical Memorandum NMFS-NWFSC-65.
9. Foote, K. G., 1985. Rather-high-frequency sound scattering by swimbladdered fish. *J. Acoust. Soc. Am.*, 78: 688–700.
10. Gauthier, S. and Rose, G.A., 2002. *In situ* target strength studies on Atlantic redfish (*Sebastes* spp.). *ICES J. Mar. Sci.*, 59: 805-815.
11. Grandin, C. J., Johnson, K. F., Edwards, A. M., Berger, A. M., 2024. Status of the Pacific Hake (whiting) stock in U.S. and Canadian waters in 2024. Prepared by the Joint Technical Committee of the U.S. and Canada Pacific Hake/Whiting Agreement, National Marine Fisheries Service and Fisheries and Oceans Canada. 246 p.
12. Henderson, M. J. and Horne, J. K., 2007. Comparison of in situ, ex situ, and backscatter model estimates of Pacific hake (*Merluccius productus*) target strength. *Can. J. Fish. Aquat. Sci.* 64: 1781-1794.
13. Horowitz, J. L., 2019. Bootstrap methods in econometrics. *Annual Review of Economics.* 11: 193–224.
14. Jones, H. L., 1974. Jackknife estimation of functions of stratum mean. *Biometrika.* 61: 343–348. doi:10.2307/2334363. JSTOR 2334363.
15. Johnson, K.F., A.M. Edwards, A.M. Berger, and C.J. Grandin, 2021. Status of the Pacific Hake (whiting) stock in U.S. and Canadian waters in 2021. Prepared by the Joint Technical Committee of the U.S. and Canada Pacific Hake/Whiting Agreement, National Marine Fisheries Service and Fisheries and Oceans Canada.
16. Kloser, R. J., Ryan, T. E., Macaulay, G. J., and Lewis, M. E., 2011. *In situ* measurements of target strength with optical and model verification: a case study for blue grenadier, *Macruronus novaezelandiae*. 68: 1986-1995.

17. Lauffenburger, N., De Robertis, A., and Williams, K. 2023. Mining previous acoustic surveys to improve walleye pollock (*Gadus chalcogrammus*) target strength estimates. *ICES Journal of Marine Science*, 0: 1–14. <https://doi.org/10.1093/icesjms/fsad094>
18. Longo, G.C., Head, M., Parker-Stetter, S., Taylor, I., Tuttle, V., Billings, A., Gauthier, S., McClure, M., Nichols, K.M. 2024. Population genomics of coastal Pacific Hake (*Merluccius productus*). *North American Journal of Fisheries Management*, 44:222–234 <https://doi.org/10.1002/nafm.10969>
19. Love, R. H., 1978. Resonant acoustic scattering by swimbladder-bearing fish. *J. Acoust. Soc. Am.* 64: 571–580.
20. McClatchie, S., Alsop, J., and Coombs, R. F. 1996. A re-evaluation of relationships between fish size, acoustic frequency and target strength. *ICES Journal of Marine Science*, 53: 780–791.
21. McClatchie, S., Macaulay, G. J., and Coombs, R. F. 2003. A requiem for the use of  $20 \log(10)$  length for acoustic target strength with special reference to deep-sea fishes. *ICES Journal of Marine Science*, 60: 419–428.
22. Madirolas, A., Membiela, F. A., Gonzalez, J. D., Cabreira, A. G., dell'Erba, M., Prario, I. S., and Blanc, S., 2017. Acoustic target strength (TS) of argentine anchovy (*Engraulis anchoita*): the nighttime scattering layer. *ICES J. Mar. Sci.*, 74: 1408–1420.
23. Medwin, H. and Clay, C. S., 1998. Fundamentals of Acoustic Oceanography, Academic Press, <https://doi.org/10.1016/B978-0-12-487570-8.X5000-4>.
24. Morse, P. H. and Ingard, U., 1968. Theoretical Acoustics. McGraw-Hill, New York.
25. Ona, E. (ed), 1999. Methodology for Target Strength Measurements (With special reference to *in situ* techniques for fish and mikro-nekton). ICES Cooperative Research Report No. 235. 59 pp.
26. Pedersen, G., Godø, O. R., Ona, E. and Macaulay, G. J. 2011. A revised target strength–length estimate for blue whiting (*Micromesistius poutassou*): implications for biomass estimates, *ICES Journal of Marine Science*, Volume 68 (10): 2222–2228. <https://doi.org/10.1093/icesjms/fsr142>
27. Peña, H., 2008. *In situ* target-strength measurements of Chilean jack mackerel (*Trachurus symmetricus murphyi*) collected with a scientific echosounder installed on a fishing vessel. *ICES J. Mar. Sci.*, 65: 594–604.
28. Rose, G. A. and Porter, D. R. 1996. Target-strength studies on Atlantic cod (*Gadus morhua*) in Newfoundland waters, *ICES Journal of Marine Science*, Volume 53 (2): 259–265. <https://doi.org/10.1006/jmsc.1996.0032>
29. Simmonds, J. and MacLennan, D.N., 2005. Fisheries Acoustics: Theory and Practice. 2nd Ed. Blackwell Publishing, London ISBN: 978-0-632-05994-2.
30. Scherbino, M. and Truskanov, M. D., 1966. Determination of fish concentration by means of acoustic apparatus. *ICES CM 1966/F:3*, p. 6.
31. Stanton, T. K., 1988. Sound scattering by cylinders of finite length. I. Fluid cylinders, *J. Acoust. Soc. Am.*, 83: 55–63. <https://doi.org/10.1121/1.396184>
32. Stanton, T.K., (1989) Sound scattering by cylinders of finite length. III. Deformed, *J. Acoust. Soc. Am.*, 86: 691–705. <https://doi.org/10.1121/1.398193>
33. Traynor, J. J., 1996. Target-strength measurements of walleye pollock (*Theragra chalcogramma*) and Pacific whiting (*Merluccius productus*). *ICES J. Mar. Sci.* 53:253–258.
34. Winger, P.D., Eayrs, S. and Glass, C.W. 2010. Fish Behavior near Bottom Trawls. In *Behavior of Marine Fishes*, P. He (Ed.). <https://doi.org/10.1002/9780813810966.ch4>

**Disclaimer/Publisher's Note:** The statements, opinions and data contained in all publications are solely those of the individual author(s) and contributor(s) and not of MDPI and/or the editor(s). MDPI and/or the editor(s) disclaim responsibility for any injury to people or property resulting from any ideas, methods, instructions or products referred to in the content.